

## [Ni(xbsms)Ru(CO)<sub>2</sub>Cl<sub>2</sub>]: A Bioinspired Nickel–Ruthenium Functional Model of [NiFe] Hydrogenase

Y. Oudart,<sup>†</sup> V. Artero,<sup>\*†</sup> J. Pécaut,<sup>‡</sup> and M. Fontecave<sup>†</sup>

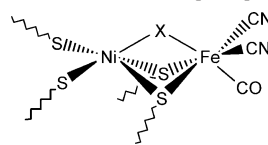
Laboratoire de Chimie et Biochimie des Centres Rédox Biologiques UMR CNRS-UJF-CEA 5047, DRDC/CB, and Service de Chimie Inorganique et Biologique, DRFCM/SCIB, CEA-Grenoble Bat K' 17 rue des Martyrs, 38054 Grenoble Cedex 9, France

Received March 27, 2006

As a model of the active site of [NiFe] hydrogenases, a dinuclear nickel–ruthenium complex [Ni(xbsms)Ru(CO)<sub>2</sub>Cl<sub>2</sub>] was synthesized and fully characterized. The three-dimensional structure reveals a nickel center in a square-planar dithioether–dithiolate environment connected to a ruthenium moiety via a Ni( $\mu$ -SR)<sub>2</sub>Ru bridge. This complex catalyzes hydrogen evolution by electroreduction of the weakly acidic Et<sub>3</sub>NH<sup>+</sup> ions in *N,N*-dimethylformamide and is therefore the first functional bioinspired model of [NiFe] hydrogenases.

Hydrogenases are enzymes that catalyze the reversible formation/oxidation of dihydrogen. They are of major environmental and potential industrial importance in the context of the development of a clean and sustainable hydrogen economy. Among them, [NiFe] hydrogenases form a specific class of metalloenzymes containing a dinuclear nickel–iron active center as shown in Chart 1. In the reduced active state, the nickel ion is coordinated by four cysteine residues, with two of them also bridging a {Fe(CO)(CN)<sub>2</sub>} moiety.<sup>1</sup>

[NiFe] hydrogenase from *Chromatium vinosum* displays a Nerstian catalytic behavior for hydrogen oxidation and thus represents a possible alternative to platinum metal as a molecular catalyst for dihydrogen/proton cation interconversion.<sup>2</sup> This has prompted the synthesis of a great variety of low molecular mass dinuclear bioinspired complexes<sup>3</sup> to gain more insight into the catalytic reaction mechanism and to further develop new electrocatalysts to be used in fuel cells for hydrogen uptake or in electrolytic/photosynthetic cells for hydrogen production.<sup>4</sup> The most accurate of these

**Chart 1.** Structure of the Active Site of [NiFe] Hydrogenases<sup>a</sup>

<sup>a</sup> X is an oxygenated ligand removed upon reduction.

structural mimicks is [(dedtc)Ni(pdt)Fe(CO)<sub>2</sub>CN<sub>2</sub>]<sup>−</sup> (dedtc<sup>−</sup> = diethyldithiocarbamate anion; H<sub>2</sub>pdt = propanedithiol),<sup>5</sup> having a nickel ion in a S<sub>4</sub><sup>3−</sup> environment and both carbonyl and cyanide ligands bound to the iron. However, none of the structural mimicks described so far were shown to be catalytically active. On the other hand, the role of the carbonyl and cyanide ligands found at the active site is probably restricted to the modulation of the electronic character and the reactivity of the iron(II) center. Thus, we decided to replace the whole {Fe(CO)(CN)<sub>2</sub>} group by another electron-rich organometallic moiety such as {Ru(CO)<sub>2</sub>Cl<sub>2</sub>}. Ruthenium can easily accommodate both hard and soft ligands including dihydrogen or hydride, and carbonyl ligands help to stabilize hydride species through charge delocalization or can react through water-gas shift reaction to generate a hydride ligand.<sup>6</sup> Many ruthenium complexes as well as one diruthenium analogue of the iron-only hydrogenase active site<sup>7</sup> are known to catalytically activate hydrogen.<sup>8</sup> Most of these ruthenium catalysts bear diphosphine, diimine, or diamine ligands, but since Darensbourg et al. showed that {NiN<sub>2</sub>S<sub>2</sub>} moieties can serve as ligands in the same way as diimines and diphosphines,<sup>9</sup> it was tempting to use such moieties to prepare and investigate nickel–ruthenium complexes. We describe here the synthesis

\* To whom correspondence should be addressed. E-mail: vartero@cea.fr.

<sup>†</sup> Laboratoire de Chimie et Biochimie des Centres Rédox Biologiques.

<sup>‡</sup> Service de Chimie Inorganique et Biologique.

(1) Volbeda, A.; Fontecilla-Camps, J. C. *Dalton Trans.* **2003**, 4030.

(2) Jones, A. K.; Sillery, E.; Albracht, S. P. J.; Armstrong, F. A. *Chem. Commun.* **2002**, 866.

(3) (a) Bouwman, E.; Reedijk, J. *Coord. Chem. Rev.* **2005**, 249, 1555.

(b) Marr, A. C.; Spencer, D. J. E.; Schröder, M. *Coord. Chem. Rev.* **2001**, 219–221, 1055.

(4) Artero, V.; Fontecave, M. *Coord. Chem. Rev.* **2005**, 249, 1518.

(5) Li, Z.; Ohki, Y.; Tatsumi, K. *J. Am. Chem. Soc.* **2005**, 127, 8950.

(6) Goicoechea, J. M.; Mahon, M. F.; Whittlesey, M. K.; Kumar, P. G. A.; Progosin, P. S. *Dalton Trans.* **2005**, 588.

(7) Justice, A. K.; Linck, R. C.; Rauchfuss, T. B.; Wilson, S. R. *J. Am. Chem. Soc.* **2004**, 126, 13214.

(8) Jessop, P. G.; Ikariya, T.; Noyori, R. *Chem. Rev.* **1995**, 95, 259. Jessop, P. G.; Joó, F.; Tai, C.-C. *Coord. Chem. Rev.* **2004**, 248, 2425. Noyori, R.; Hashiguchi, S. *Acc. Chem. Res.* **1997**, 30, 97. Hayashi, H.; Ogo, S.; Fukuzumi, S. *Chem. Commun.* **2004**, 2714.

(9) Rampersad, M. V.; Jeffery, S. P.; Golden, M. L.; Lee, J.; Reibenspies, J. H.; Darensbourg, D. J.; Darensbourg, M. Y. *J. Am. Chem. Soc.* **2005**, 127, 17323.

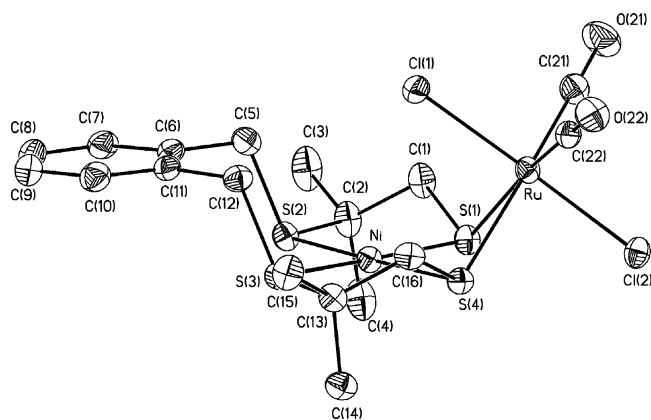


**Figure 1.** Structure of **1** in 1·2CHCl<sub>3</sub> (30% probability thermal ellipsoids; crystallographic data are given in Tables S1 and S2 in the Supporting Information). Selected bond lengths (Å) and angles (deg): Ru–C(21) 1.881(5), Ru–C(22) 1.883(4), Ru–Cl(1) 2.4040(10), Ru–Cl(2) 2.4085(10), Ru–S(1) 2.4423(11), Ru–S(4) 2.4481(10), Ni–S(1) 2.1864(11), Ni–S(4) 2.1886(11), Ni–S(2) 2.2118(11), Ni–S(3) 2.2134(11), C(21)–Ru–C(22) 91.89(18), C(21)–Ru–Cl(1) 88.42(13), C(22)–Ru–Cl(1) 90.73(12), C(21)–Ru–Cl(2) 91.63(13), C(22)–Ru–Cl(2) 91.44(12), Cl(1)–Ru–Cl(2) 177.83(4), C(21)–Ru–S(1) 100.13(14), C(22)–Ru–S(1) 167.81(12), Cl(1)–Ru–S(1) 91.60(4), Cl(2)–Ru–S(1) 86.26(4), C(21)–Ru–S(4) 172.94(14), C(22)–Ru–S(4) 95.17(12), Cl(1)–Ru–S(4) 91.39(4), Cl(2)–Ru–S(4) 88.29(4), S(1)–Ru–S(4) 72.82(3), S(1)–Ni–S(4) 83.13(4), S(1)–Ni–S(2) 91.97(4), S(4)–Ni–S(2) 175.10(4), S(1)–Ni–S(3) 174.70(4), S(4)–Ni–S(3) 92.09(4), S(2)–Ni–S(3) 92.81(4).

of a novel heterodinuclear nickel–ruthenium complex [Ni(xbsms)Ru(CO)<sub>2</sub>Cl<sub>2</sub>] [**1**; H<sub>2</sub>xbsms = 1,2-bis(4-mercapto-3,3-dimethyl-2-thiabutyl)benzene], which catalyzes triethylammonium electroreduction with hydrogen evolution at –1.60 V vs Ag/AgCl on a mercury pool in *N,N*-dimethylformamide (DMF) and can thus be considered as the first functional bioinspired model of [NiFe] hydrogenases.

Stoichiometric reaction of [Ni(xbsms)]<sup>10</sup> with [RuCl<sub>2</sub>(CO)<sub>2</sub>]<sub>*n*</sub><sup>11</sup> in CH<sub>2</sub>Cl<sub>2</sub> under argon affords the dinuclear complex **1** with good yield. IR spectroscopy analysis of the solution 5 min after mixing of the reactants shows that **1** is the only carbonyl-containing species with IR absorptions at 2053 and 1990 cm<sup>-1</sup>. Purification through column chromatography yields an analytically pure compound.

The structure of the dinuclear complex **1** is shown in Figure 1.<sup>12</sup> The nickel atom is in a square-planar environment formed by the four sulfur atoms. [Ni(xbsms)] binds the ruthenium ion as a bidentate sulfur-donor ligand. The nickel–ruthenium distance is 3.19 Å. Because of steric interaction with the axial methyl groups of the Ni(xbsms) fragment, the ruthenium moiety is located trans to the axial methyl groups and therefore cis with the aromatic cycle of the xbsms ligand. The hinge angle typical for thiolate-bridged dinuclear complexes<sup>9</sup> between the NiS<sub>4</sub> and RuS<sub>2</sub>(CO)<sub>2</sub> planes is 124.1°, indicating that the methylene groups adjacent to sulfur atoms provide significant steric hindrance to the {Ru(CO)<sub>2</sub>Cl<sub>2</sub>} unit. Cl(1) is directed toward but does not interact

with the nickel atom [*d*(Cl⋯Ni) = 3.15 Å]. The ruthenium atom is in an octahedral environment with three pairs of similar ligands. Significant distortion in the equatorial plane of the ruthenium octahedra arises from the acute S1–Ru–S4 angle [72.82(3)°] as a result of bridging constraints. The carbonyl ligands are cis with respect to each other. The same relative arrangement is observed for thiolate ligands, while the chloride ligands are located trans to each other. Bond lengths are similar within all three pairs. The same octahedral arrangement with both carbonyl trans to thiolate ligands and cyanide in a trans configuration is observed around the iron atom in [(dedtc)Ni(pdt)Fe(CO)<sub>2</sub>(CN)<sub>2</sub>]<sup>-</sup>.<sup>5</sup> Such a stereochemical arrangement optimizes electronic transfer from sulfur lone pairs toward π-acceptor carbonyl ligands through ruthenium orbitals.

<sup>1</sup>H and <sup>13</sup>C NMR spectra of **1** indicate a C<sub>s</sub> symmetry with heterotopic faces for the xbsms ligand. Carbonyl ligands in **1** are equivalent and display one signal at 194 ppm in CDCl<sub>3</sub>. This indicates that the solid-state molecular structure is retained in solution.

The cyclic voltammogram of **1** recorded on a glassy carbon electrode vs Ag/AgCl/KCl (3 mol·L<sup>-1</sup>) in DMF shows a reversible one-electron redox process at +0.64 V, which could be assigned to the nickel(III)/nickel(II) couple by comparison with the cyclic voltammogram of [Ni(xbsms)] recorded under the same conditions (+0.65 V, Figure S1 in the Supporting Information). The cyclic voltammogram also displays an irreversible two-electron reduction peak at –0.90 V. The chemical reaction responsible for irreversibility is not identified yet. Loss of chloride and/or carbonyl ligands from the ruthenium center is most likely. Indeed, we rule out breakdown of the binuclear species into two pieces because the electrochemical waves characteristic for [Ni(xbsms)] or [Ru(CO)<sub>2</sub>Cl<sub>2</sub>]<sub>*n*</sub> are not observed in the reverse and subsequent scans.

Upon addition of 1.5 equiv of Et<sub>3</sub>NH<sup>+</sup> to a DMF solution of **1**, a new irreversible cathodic wave appears at –1.50 V. It rises in height and shifts to more negative potentials when the acid/catalyst concentration ratio is increased, as shown in Figure 2. This wave has thus an electrocatalytic behavior<sup>13</sup> and can be assigned to proton electroreduction.

Hydrogen evolution is observed during electrolysis (Figure 3) of 0.45 mmol of Et<sub>3</sub>NHCl on a mercury pool at –1.60 V vs Ag/AgCl in DMF (10 mL) in the presence of 15 μmol of **1** as the electrocatalyst. Remarkably, the substrate is quantitatively converted to dihydrogen (15 turnovers) in 3 h. Under the same conditions but in the absence of a catalyst, less than 5% of Et<sub>3</sub>NH<sup>+</sup> is converted to dihydrogen within the same reaction time. Two new additions of 0.45 mmol of Et<sub>3</sub>NHCl allow successive electrolytic runs for a total turnover number of 45, thus with comparable yield. The reaction, however, is slightly slower, indicating some degradation of the catalyst during catalysis. Hydrogen is also produced when the former solution is electrolyzed at a potential just required to reduce **1** (–1.2 V vs Ag/AgCl). The rate is 3 times slower in this case.

(13) Razavet, M.; Artero, V.; Fontecave, M. *Inorg. Chem.* **2005**, *44*, 4786 and references cited therein.

(10) Verhagen, J. A. W.; Ellis, D. D.; Lutz, M.; Spek, A. L.; Bouwman, E. *Dalton Trans.* **2002**, 1275.

(11) Cleare, M. J.; Griffith, W. P. *J. Chem. Soc. A* **1969**, 372. Grocott, S. C.; Wild, S. B. *Inorg. Chem.* **1982**, *21*, 3535.

(12) CCDC 281930 contains the supplementary crystallographic data for this paper. These data can be obtained free of charge from the Cambridge Crystallographic Data Center via [www.ccdc.cam.ac.uk/dataservice/cif](http://www.ccdc.cam.ac.uk/dataservice/cif).

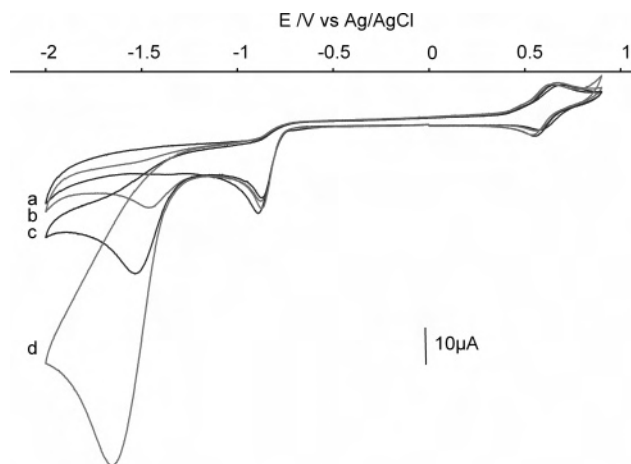


**Figure 2.** Cyclic voltammograms of **1** ( $1.0 \text{ mmol}\cdot\text{L}^{-1}$ ) in the presence of various amounts of  $\text{Et}_3\text{NHCl}$  recorded in a DMF solution of  $n\text{-Bu}_4\text{NBF}_4$  ( $0.1 \text{ mol}\cdot\text{L}^{-1}$ ) on a glassy carbon electrode at  $100 \text{ mV}\cdot\text{s}^{-1}$ : (a) 0 equiv; (b) 1.5 equiv; (c) 3.0 equiv; (d) 10 equiv.

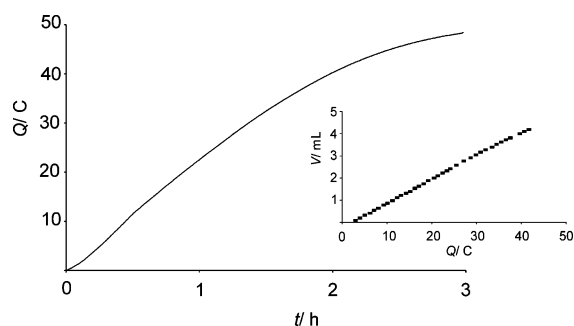


**Figure 3.** Coulometry for bulk electrolysis at  $-1.60 \text{ V}$  vs  $\text{Ag}/\text{AgCl}$  of a DMF solution ( $10 \text{ mL}$ ) of  $\text{Et}_3\text{NHCl}$  ( $0.45 \text{ mmol}$ ) and  $n\text{-Bu}_4\text{NBF}_4$  ( $0.1 \text{ mol}\cdot\text{L}^{-1}$ ) on a mercury pool in the presence of **1** ( $15 \mu\text{mol}$ ). Under these conditions, 1 TON corresponds to 2.89 C. The volume of the evolved hydrogen as a function of the charge is represented in the inset.

The active species is likely to be a metal–hydride compound resulting from the reaction of protons with a reduced binuclear complex. However, the fact that the catalytic wave develops at potentials lower than that required for the initial reduction of **1** suggests that this metal–hydride species should be further reduced for activation. Such a mechanism has already been proposed by Savéant et al. for proton electroreduction catalyzed by a rhodium porphyrin.<sup>14</sup> It is thus clear that **1** is not the catalyst per se but rather a precursor of the stable catalytically active complex capable of multiple turnovers. Further work is needed to characterize it.<sup>15</sup>

(14) Grass, V.; Lexa, D.; Savéant, J.-M. *J. Am. Chem. Soc.* **1997**, *119*, 7526.

**1** is thus the first bioinspired binuclear model of  $[\text{NiFe}]$  hydrogenases with interesting catalytic activity for hydrogen evolution. One major drawback so far is still the high activation potential, yet in the same range of those of other nickel complexes such as  $[\text{Ni}_2(\text{bis-cyclam})]^{4+}$  active in neutral conditions.<sup>4,16</sup> However, **1** still lacks two important structural features found at the active site of  $[\text{NiFe}]$  hydrogenases.<sup>4</sup> First, a strong distortion from either tetrahedral or square-planar geometry is observed at the active site of  $[\text{NiFe}]$  hydrogenases. DuBois et al. have pointed out the fundamental effects of the tetrahedral distortion of nickel complexes on their hydride acceptor ability.<sup>17</sup> Second, all of the heterodinuclear mimicks described so far lack a built-in basic site, whereas theoretical calculations propose that one of the nonbridging cysteinate ligands of the nickel in the active site of the  $[\text{NiFe}]$  hydrogenases mediates proton transfer to a metal–hydride intermediate, resulting in the formation of dihydrogen coordinated to iron.<sup>18,19</sup> Despite the  $\text{S}_4$  environment around the nickel ion, the two thiolate ligands in **1** are already engaged in the  $\text{Ni}(\mu\text{-SR})_2\text{Ru}$  bridge and the two thioether functions are not reactive toward protonation. Further work, devoted to the improvement of the catalytic properties of such bioinspired models, will thus include both the synthesis of original  $\text{S}_4$  ligands, avoiding square-planar coordination with at least three thiolate ligation sites, and the search for new organometallic moieties working in synergy with the nickel center.

**Acknowledgment.** This research was supported through the Biohydrogen Program by the Life Sciences Division of the CEA. The authors thank Nicolas Duraffourg for performing NMR correlation experiments.

**Supporting Information Available:** Experimental details of synthesis, spectroscopic characterizations,  $[\text{Ni}(\text{xbsms})]$  (Figure S1) and blank cyclic voltammograms, and crystallographic data (Tables S1 and S2 and in CIF format). This material is available free of charge via the Internet at <http://pubs.acs.org>.

IC060510F

- (15) Any heterogeneous catalysis (coating or amalgam) is also ruled out because neither the mercury pool nor the graphite electrode exhibits catalytic activity when washed after electrochemical experiments and replaced under the same conditions in the absence of a catalyst. The electrolytic solution remains clear after catalysis.
- (16) Collin, J.-P.; Jouaiti, A.; Sauvage, J.-P. *Inorg. Chem.* **1998**, *27*, 1986.
- (17) Curtis, C. J.; Miedaner, A.; Ciancanelli, R.; Ellis, W. W.; Noll, B. C.; DuBois, M. R.; DuBois, D. L. *Inorg. Chem.* **2003**, *42*, 216.
- (18) Stein, M.; Lubitz, W. *Curr. Opin. Chem. Biol.* **2002**, *6*, 243.
- (19) Niu, S.; Hall, M. B. *Inorg. Chem.* **2001**, *40*, 6201. Siegbahn, P. E. M.; Blomberg, M. R. A.; Wirstam née Pavlov, M.; Crabtree, R. H. *J. Biol. Inorg. Chem.* **2001**, *6*, 460 and references cited therein.